ICARUS **130,** 259–274 (1997)
ARTICLE NO. IS975821

Assessment of Kinetic Energy of Meteoroids Detected by Satellite-Based Light Sensors

I. V. Nemtchinov, V. V. Svetsov, I. B. Kosarev, A. P. Golub', O. P. Popova, and V. V. Shuvalov

Institute for Dynamics of Geospheres, Russian Academy of Sciences, 38 Leninskii Prospect (Building 6), Moscow 117979, Russia

R. E. Spalding and C. Jacobs

Sandia National Laboratories, Organization 5909, MS 0978, P.O. Box 5800, Albuquerque, New Mexico 87185
E-mail: respald@sandia.gov

and

E. Tagliaferri

E.T. Space Systems, 5990 Worth Way, Camarillo, California 93012

Received July 29, 1996; revised August 18, 1997

Radiation energies of bright flashes caused by disintegration of large meteoroids in the atmosphere have been measured using optical sensors on board geostationary satellites. Light curves versus time are available for some of the events. We have worked out several numerical techniques to derive the kinetic energy of the meteoroids that produced the flashes. Spectral opacities of vapor of various types of meteoroids were calculated for a wide range of possible temperatures and densities. Coefficients of conversion of kinetic energy to radiation energy were computed for chondritic and iron meteoroids 10 cm to 10 m in size using radiation–hydrodynamics numerical simulations. Luminous efficiency increases with body size and initial velocity. Some analytical approximations are presented for average conversion coefficients for irons and H-chondrites. A mean value of this coefficient for large meteoroids (1–10 m in size) is about 5–10%. The theory was tested by analyzing the light curves of several events in detail.

Kinetic energies of impactors and energy–frequency distribution of 51 bolides, detected during 22 months of systematic observations in 1994–1996, are determined using theoretical values of luminous efficiencies and heat-transfer coefficients. The number of impacts in the energy range from 0.25 to 4 kt TNT is 25 per year and per total surface of the Earth.

The energy–frequency distribution is in a rather good agreement with that derived from acoustic observations and the lunar crater record. Acoustic systems have registered one 1 Mt event in 12 years of observation. Optical systems have not detected such an event as yet due to a shorter time of observation. The probability of a 1 Mt impact was estimated by extrapolation of the observational data.

1. INTRODUCTION

A relatively small number of satellites in high-altitude orbits (20,000 km and higher) provide coverage of most of the Earth's surface. It is possible to have essentially continuous, 24-h, all weather coverage over the entire surface of the Earth. Space-based infrared sensors detect bright flashes (the average number of flashes is about 30 per year). In addition, optical sensors detect light curves in the visible portion of the spectrum. The bright flashes are caused by explosive disintegration of large meteoroids in the atmosphere (Reynolds 1992, Tagliaferri 1993, 1996, Tagliaferri *et al.* 1994, McCord *et al.* 1995).

Information that can be derived from observations by the Satellite Network (SN) is of great interest to planetary science. Energy–frequency distribution of SN bolides may provide the opportunity to predict probability of impacts, give a more accurate account of the population of the near-Earth objects, and anticipate the hazard from large impacts.

Retrieval of meteoroid attributes (energy, velocity, mass, density) from the light power curves is a challenging task. The simplest method to assess the meteoroid kinetic energy is to divide the released radiation energy by a luminous efficiency (efficiency for conversion of kinetic energy to radiation energy). The use of empirical values of luminous efficiency for small meteoroids (Bronsten 1983) and artificial meteors (Ayers *et al.* 1970, Givens and Page 1971) is inappropriate for assessment of large SN meteoroids. The luminous efficiencies derived for large Prairie Network

0019-1035/97 $25.00

and European Network bolides (ReVelle and Rajan 1979, ReVelle 1979, 1980) may also be unsuitable because the masses of the meteoroids detected from the satellites might be by two or three orders of magnitude higher. An increase in the geometrical and optical thicknesses of the shock-heated air and vapor layers may substantially increase the radiation fluxes and the values of luminous efficiency. On the other hand, values of conversion efficiency for the nuclear fireball (30–70%) obtained in the course of nuclear testing (Glasstone and Dolan 1977) and in calculations (Svetsov 1994) are inapplicable because of a substantial difference in the energy release, shape, and size of the radiating volumes.

An average conversion efficiency of 5–10% assumed in Reynolds (1992) and in McCord *et al.* (1995) for bolides detected from the satellites seems to be a reasonable interpolation but is poorly justified. A related problem is that the real light power of Satellite Network events is unknown. This power is reconstructed with the assumption of 6000 K effective temperature of the fireball (Tagliaferri *et al.* 1994, McCord *et al.* 1995). This assumption undoubtedly introduces errors (McCord *et al.* 1995).

Estimates of sizes and masses of 21 SN bolides have been given by Ceplecha *et al.* (1996). Empirical values of luminous efficiencies were derived from the dynamical trajectory analysis of 43 PN bolides. We should note that the spectrum of the bolide depends on the meteoroid size, velocity, height of flight, and composition. Different detector types will have differing sensitivities at various wavelengths. Luminous efficiencies determined in the panchromatic bandpass of the ground-based photographic observational system may differ substantially from that of the silicon photoelectric detector which has been used in the satellite-based network (Tagliaferri *et al.* 1994).

We have developed some purely theoretical methods of estimating meteoroid characteristics and carried out numerical simulations of meteoroid flight and ablation to obtain the conversion efficiency. First, we calculated tables of optical properties of the vapor. To the best of our knowledge, there were no data on opacities of the vapor of meteoroid material in the literature. Second, using these tables, we have computed self-consistent values of the heat transfer coefficients and coefficients of conversion of kinetic energy into radiation energy for a single body with constant radius. Earlier, heat transfer coefficients had been calculated by Biberman *et al.* (1980) for man-made bodies with a heat shield cover. Those values are substantially smaller than empirical coefficients commonly used in meteor physics (Bronsten 1983). This contradiction was an additional reason for our computations for irons and chondrites.

An analysis of light curves of some of the events show that a theory based on assumption of a constant or diminishing (due to ablation) radius of the meteoroid cannot explain sharp increases in the light power. But assumption of an increasing effective radius of the meteoroid leads to a good agreement with the observational light curves (Svetsov *et al.* 1995), so we employed a theory of a ''pancake'' impactor expansion suggested by Zahnle (1992) and Chyba *et al.* (1993).

We have computed radiation impulses of the meteoroids for various possible compositions and strengths of the body. Some approximation has been derived for bolides with kinetic energy higher than about 10 t TNT. This provides a possibility for determining kinetic energy of the SN bolides, i.e., those detected by satellites. An ultimate purpose of the work is to determine an energy–frequency distribution of meteoroids. Preliminary results for 21 events detected during 1994 and a month and a half of 1995 have been given in Nemtchinov *et al.* (1996b). We have also analyzed a large number of other events detected during 1995 and the first three months of 1996. Statistics are still rather poor, especially for low- and high-energy events; nevertheless, our analysis provides an opportunity to estimate the flux of meteoroids, at least in the initial kinetic energy range from 0.25 to 4 kt TNT using the data from systematic observations over approximately 2 years.

2. OPACITIES OF METEOROID VAPOR

Meteoroids have various compositions. They can be iron, chondrite, carbonaceous chondrite, or cometary bodies. The chondrites alone have a composition that differs substantially among the various types. To complicate the situation, the chemical composition of comets is also very uncertain. Calculations of optical properties of various types of meteoroids are important for providing a more penetrating insight into the meteoric phenomena. We have completed computations of the optical properties of irons, H-, L- and LL-chondrites and carbonaceous chondrites, cometary material with composition of Comet Halley, and pure icy bodies. Here we present and compare data only for irons and H-chondrites.

The composition of H-chondrite was taken from the review of Jarocewich (1990), i.e., 36.6% SiO_2, 23.3% MgO, 10.3% FeO, 16.0% Fe, and 5.4% FeS. Computations of vapor composition (defined by thermodynamic equilibrium of chemical reactions) and absorption coefficients were carried out for temperatures from 2000 to 40,000 K. Densities of the vapor varied from 1×10^{-8} g/cm^3 to 1×10^{-2} g/cm^3. Chemical composition is modeled by compounds of 10-elements system (Fe–O–Mg–Si–C–H–S–Al–Ca–Na) and their subsystems. The total number of components is 167. The following components of H-chondrite vapor were taken into account: SiO_2, SiO, SiO^+, Si_2, Si_2^+, Si, Si^-, $Si^+ \ldots Si^{6+}$, MgO, Mg, $Mg^+ \ldots Mg^{6+}$, O_2, O_2^-, O_2^+, O, O^-, $O^+ \ldots O^{6+}$, FeO, FeO^-, Fe, Fe^-, Fe_2^-, Fe_2^+, $Fe^+ \ldots Fe^{6+}$, atoms and ions of sulfur, sodium, calcium, alu-

minum, and e. At lower temperatures H_2O, CO_2, CO, CO_2^+, CO^+, SO_2, SO, OH, CH, AlO, Na_2, Na_2O, CaO, CaH, FeH, MgH, SiH, and many others were included.

Iron-body vapor was described through the following components: Fe_2, Fe_2^+, Fe_2^-, Fe^-, and FeI–FeVI.

Details of calculations are described in Golub' *et al.* (1996) and Kosarev *et al.* (1996). Figure 1 illustrates the behavior of linear absorption coefficients of H-chondrite vapor. Most of the lines are concentrated at photon energies less than 8 eV.

A 1-cm vapor layer is found to be opaque for photons in the range of 2–3 eV and higher. This means that a meteoroid surface will be at least partially screened by the vapor layer. Absorption of the radiation coming from the shock heated air substantially increases the temperature of the vapor above the temperature of phase transition that is equal to about 3000 K both for iron and H-chondrite (Baldwin and Sheaffer 1971, Remo 1994). Opacities of H-chondrite are dominated by a multitude of spectral lines, mainly iron atoms and ions. Iron atoms and ions appear after iron oxide dissociation at a temperature of some thousands.

3. HEAT TRANSFER AND ENERGY CONVERSION COEFFICIENTS

A direct but very complex and time-consuming way to calculate the coefficients of heat transfer and energy conversion is to solve a 3D radiation–hydrodynamic problem for flow around an ablating body. Ablation, i.e., vaporization and melting, presents a considerable challenge to the numerical methods. Several scales, instabilities, and turbulent mixing make the problem more complicated.

Heat transfer coefficients were computed by Biberman *et al.* (1980) for a body covered by heat shielding material using some simplifications. Radiation transfer was computed in a 1D planar layer that is a first-order approximation to the shock-heated cap around the leading face of a blunt body. Here we compute heat-transfer coefficients and energy-conversion coefficients also exploiting 1D geometry. But instead of a steady-state problem relevant only for the computation of the radiation flux at a stagnation point, we consider an unsteady-state problem, namely, a piston moving in the gas. We use an analogy between cylindrical explosion and flow around an axially symmetric body (Cherniy 1959, Hayes and Probstein 1959). The cylindrical piston was assumed to expand in the air, enlarging its radius with constant velocity V to radius R_p, and then return with an opposite velocity to the initial point. Work done by the piston per unit length is approximately equal to

$$W = \rho V^2 \pi R_p^2, \tag{1}$$

where ρ is the ambient air density.

The energy transferred to the air by a body of arbitrary shape with an effective radius R (per unit of trajectory length) is

$$W = \tfrac{1}{2} C_D \rho V^2 \pi R^2, \tag{2}$$

where C_D is the drag coefficient and V is the velocity of the body. Equating expressions (3) and (4), we surmise that for a spherical body ($C_D \approx 1$) R is a factor of $\sqrt{2}$ larger than the maximum radius of the equivalent piston R_p. For a cylindrical body ($C_D \approx 2$) $R_p \approx R$.

Since the velocity of the piston is equal to that of the body, temperatures in the shock-heated air are close to real temperatures around the meteoroid. Dimensions of the heated volume and characteristic times are also sufficiently close to those of 2D (or 3D) problems to give a basis for 1D modeling. Although the simplified geometry introduces some error, 1D computations of radiation transfer consume much less computer time and, hence, can be done with greater accuracy. We note that varying the velocity of the piston with time may allow approximating flow around a body with more complicated shape than a simple cylinder with plane leading edge. Some examples for blunt-nosed bodies are given in Golub' *et al.* (1996).

We have taken data on thermodynamic and optical properties of hot air from tables of Kuznetzov (1965) and Biberman (Avilova *et al.* 1970). We calculated vaporization and melting of the piston as it moves in the gas. We assumed that mass losses of the piston were approximately equal to mass losses of a meteoroid as it traverses a segment of the trajectory equal to its size. A system of equations and some details of the model are described in (Golub' *et al.* 1996) and (Nemtchinov *et al.* 1996b).

The shape of a meteoroid in this particular set of simulations is a short cone with a cylinder behind it. The radius of the blunt nose of the cone is R_b, the length of the cone is $0.4R_b$, the radius of the cylinder is $1.4R_b$, and the total length of the body is $2R_b$. The mass of this body is $M_b = 3.8\rho_b \pi R_b^3$, where ρ_b is its bulk density. The maximum cross section of the meteoroid (A) is twice the cross section of the blunt nose πR_b^2.

Principal results of our computations are shown. Table I demonstrates the heat transfer coefficients for iron and H-chondrite blunt-nosed. Heat transfer coefficients are defined here as

$$C_H = -\frac{dM}{dt}\frac{2Q_{vap}}{\rho V^3 A}, \tag{3}$$

where dM/dt is the mass losses due to ablation, ρ is the atmospheric density, V is the velocity of the meteoroid, A is the cross section, and Q_{vap} is the latent heat of vaporization (6.4 kJ/g for H-chondrite and 6.3 kJ/g for iron). Note

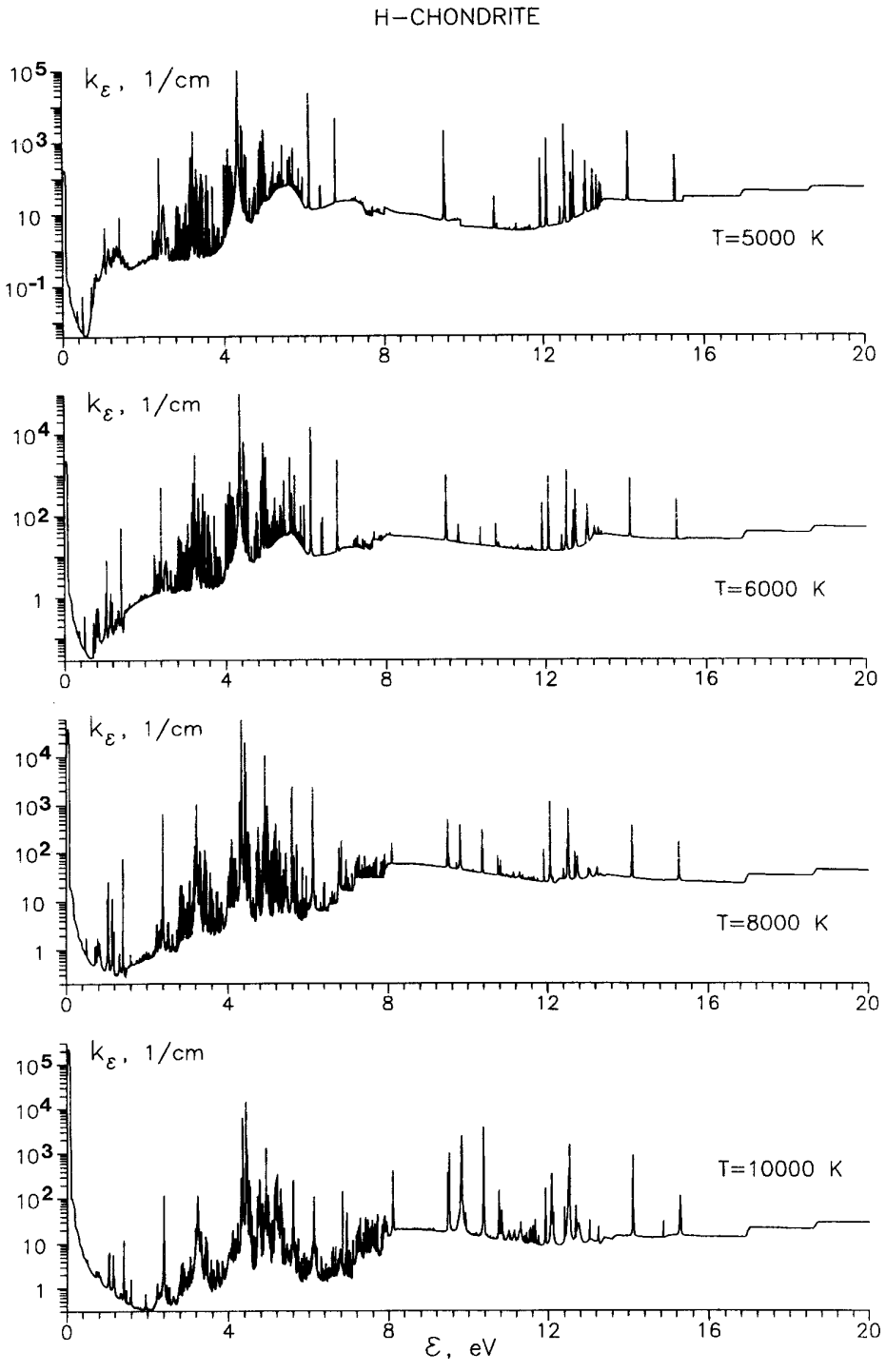

FIG. 1. Absorption coefficients K_ε of H-chondrite vapor versus photon energy ε at pressure 10 bar and temperatures T from 5000 to 10,000 K.

that we include the latent heat of vaporization in the definition of C_H, despite the fact that ablation can go into both the vaporization and melting regimes. These processes were taken into account in calculations of C_H.

The energy deposited to the atmosphere is equal to total energy losses of the meteoroid

$$\frac{dE}{dt} = MV\frac{dV}{dt} + \frac{V^2}{2}\frac{dM}{dt} = -\frac{A\rho V^3}{2}\left(C_D + C_H\frac{V^2}{2Q_{vap}}\right). \quad (4)$$

Some portion of energy is converted to radiation energy. A silicon detector has limited responsivity (Tagliaferri 1993) and absorbs a portion of released power equal to

TABLE I
Heat-Transfer Coefficient C_H

V, (km/s)	H-Chondrite, Radius R_b{m} 0.1	1	10	Iron, Radius R_b{m} 0.1	1	10
			h = 50 km			
30	0.12	0.060	0.041	0.19	0.09	0.075
20	0.14	0.075	0.060	0.26	0.13	0.12
15	0.09	0.075	0.065	0.29	0.15	0.11
10	0.10	0.049	0.029	0.09	0.14	0.06
			h = 40 km			
30	0.060	0.032	0.017	0.095	0.050	0.32
20	0.080	0.048	0.033	0.12	0.065	0.055
15	0.075	0.050	0.038	0.15	0.065	0.060
10	0.050	0.027	0.024	0.11	0.075	0.047
			h = 30 km			
30	0.026	0.014	0.007	0.041	0.022	0.012
20	0.036	0.024	0.011	0.055	0.034	0.021
15	0.041	0.032	0.016	0.070	0.040	0.025
10	0.020	0.018	0.015	0.065	0.039	0.027
			h = 20 km			
30	0.011	0.0055	0.0016	0.017	0.007	0.0029
20	0.016	0.0070	0.0023	0.025	0.010	0.0043
15	0.020	0.010	0.0036	0.033	0.013	0.0065
10	0.012	0.0095	0.0050	0.039	0.020	0.012

$$P_d = \frac{dE}{dt} f_d, \tag{5}$$

where P_d is the light power accepted by the detector, and f_d is the portion of the accepted energy.

Data on the radiated energies of light impulses released up to now (Tagliaferri *et al*. 1994, McCord *et al.* 1995) were based on energy accepted by the detector in assumption of a 6000-K blackbody source (Reynolds 1992). For that case, the radiated power that follows from the light curves is $P_r = P_d/0.4$. It is reasonable to continue using this nomenclature.

In Table II, computed values of

$$f_r = \frac{f_d}{0.4} \frac{P_r}{dE/dt} \tag{6}$$

are shown for H-chondrites and irons.

Typical spectra for H-chondrite and iron bodies are displayed in Fig. 2. The spectra differ significantly from that of a black body with temperature 6000 K. We should also underline that spectral content over the wavelength range of the DoD Satellite Network sensors, i.e., 1–3 eV, is substantially different from both that in the panchromatic spectral range or in the visible. This means that it would be erroneous to use observational data from ground-based photographic systems directly for calibration of the Satellite Network data.

4. INTEGRAL LUMINOUS EFFICIENCIES

The velocity and mass of a meteoroid diminish along the trajectory due to aerobraking and ablation as (Bronsten 1983)

$$\frac{dV}{dt} = -\frac{1}{2} C_D \rho V^2 A \tag{7}$$

$$Q \frac{dM}{dt} = -\frac{1}{2} C_H \rho V^3 A \tag{8}$$

$$\frac{dh}{dt} = -V \sin \vartheta, \tag{9}$$

where h is the altitude, and ϑ is the angle of trajectory inclination.

These equations of a single-body model are commonly used with constant or diminishing cross section. Breakup

TABLE II
Coefficient f_r of Conversion of Released Energy to Radiation Energy

V, (km/s)	H-Chondrite, Radius R_b{m} 0.1	1	10	Iron, Radius R_b{m} 0.1	1	10
			h = 50 km			
30	0.10	0.14	0.28	0.030	0.10	0.22
20	0.10	0.12	0.22	0.0068	0.080	0.18
15	0.073	0.098	0.17	0.0073	0.040	0.12
10	0.040	0.040	0.073	0.00043	0.0065	0.033
			h = 40 km			
30	0.12	0.19	0.25	0.063	0.16	0.19
20	0.11	0.14	0.24	0.045	0.14	0.19
15	0.080	0.12	0.20	0.023	0.068	0.13
10	0.028	0.040	0.078	0.0018	0.0065	0.048
			h = 30 km			
30	0.14	0.18	0.18	0.080	0.12	0.13
20	0.12	0.16	0.18	0.063	0.13	0.12
15	0.080	0.13	0.15	0.035	0.090	0.11
10	0.018	0.045	0.088	0.0050	0.017	0.065
			h = 20 km			
30	0.15	0.18	0.20	0.12	0.15	0.15
20	0.13	0.17	0.20	0.10	0.14	0.18
15	0.090	0.11	0.18	0.060	0.10	0.17
10	0.025	0.048	0.12	0.0048	0.025	0.11

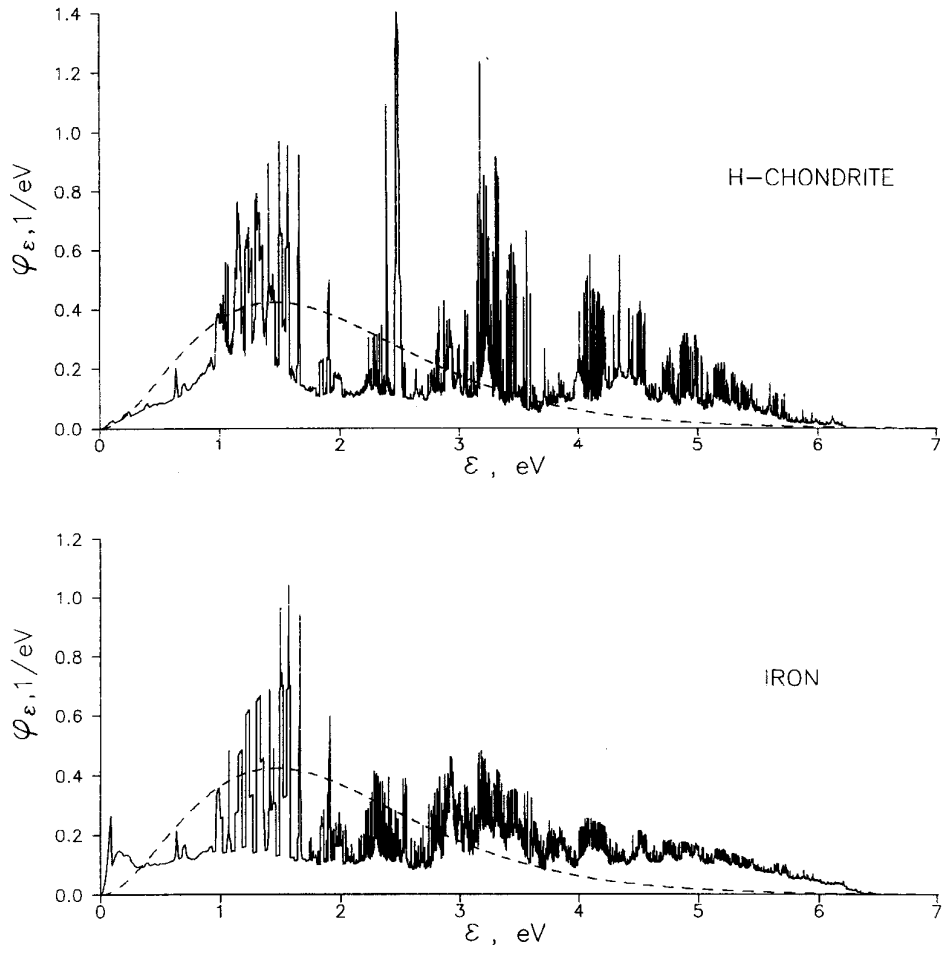

FIG. 2. Spectra of H-chondrite and iron meteoroids 1 m in radius with velocity 20 km/s at an altitude of 40 km. Spectra of a blackbody source with temperature of 6000 K are shown by dashed lines. The spectra are defined here as the light intensity divided by the integral of the intensity over photon energies.

of the bolide is a substantial feature of the meteoric phenomena. Models of a pancake impactor with a growing cross section after breakup were suggested in Zahnle (1992), Chyba *et al.* (1993), and Hills and Goda (1993).

The radius of meteoroid is assumed to grow after the breakup as

$$R\frac{d^2R}{dt^2} = \frac{C_D\rho V^2}{2\rho_b} \tag{10}$$

in the model of Chyba *et al.* (1993) and as

$$\frac{dR}{dt} = V(\rho/\rho_b)^{1/2} \tag{11}$$

in the model of Hills and Goda (1993), where ρ_b is the density of the meteoroid.

If we assume some apparent strength of the body σ and further assume that the breakup occurs when

$$\rho V^2 = \sigma, \tag{12}$$

we can compute variation of V, M, and R through a system of Eqs. (4) and (6)–(10) and compute a radiated power P_r using values of $f_r(V, R, \rho)$ from Table II. Integrating P_r over time, we get the radiative energy E_r.

Let us define integral luminous efficiency accepted by the detector as

$$\eta = \frac{E_r}{E}, \tag{13}$$

where E is the preentry kinetic energy of the meteoroid.

Using the system of Eqs. (4) and (6)–(10) we have made

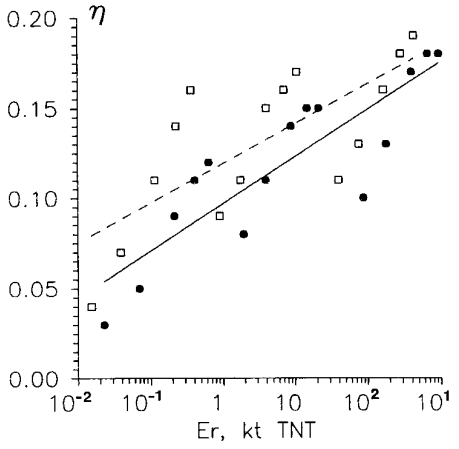

FIG. 3. Dependence of luminous efficiency η on radiated energy E_r for H-chondrite (open squares) and iron (black squares) bodies with sizes 1, 3, and 10 m and velocities 12, 15, 20, 25, 30 km/s. Dashed and solid lines are least-error approximations of integral luminous efficiency for H-chondrites and irons correspondingly. Apparent strength was assumed to be 100 Mdyn/cm^2.

computations for a range of initial parameters: velocity V from 12 to 30 km/s, initial radius R_b from 10 cm to 10 m, angle ϑ of trajectory inclination from 30 to 60^0, and yield strength σ from 30 to 200 Mdyn/cm^2. Velocity and size exert the strongest influence on P_r and η.

In Fig. 3, values of η for some variants of H-chondrites and irons are plotted as a function of the energy of the light flash.

The following approximations of η can be used

$$\eta = 0.021 \log E_r + 0.0031V + 0.037 \quad \text{(for iron)} \tag{14}$$

$$\eta = 0.021 \log E_r + 0.0055V + 0.022 \quad \text{(for H-chondrite)}, \tag{15}$$

where the velocity V is in km/s, and energy of the flash E_r is in kt TNT.

With the exception of one event (February 1, 1994), we do not know the initial velocity. The following averaged value of conversion coefficient for H-chondrites can be used in these cases

$$\eta_i = 0.021 \log E_r + 0.103. \tag{16}$$

The values of η are much smaller than those for spherical explosions of the same yield (Glasstone and Dolan 1977, Svetsov 1994). This is due to a difference in the shape of the luminous volume and gradual release of the meteoroid energy into the atmosphere.

An error in η, if expression (16) for averaged values is used, can reach a factor of 2 for high velocities or small sizes of meteoroids.

Application of pancake models (10) and (11) to large meteoroids seems to be rather well substantiated by theory. Fragmentation of such bodies begins at lower pressures than of smaller ones as it is easier to find a crack or a fault in a large body. Fragments with high masses decelerate less and experience higher stresses and they continue to fragment. Smaller fragments rapidly evaporate. Vapor fills the volume between fragments and helps to support a common shock wave comprising the fragments and vapor cloud. Fragmentation models of Hills and Goda (1993) and Svetsov (1996a,b) predict that for a Tunguska-sized body the largest fragment size is under 10 cm. A heavily fragmented mass can be treated as a fluid.

Direct numerical simulations of the flight of a "fluid" meteoroid (MacLow and Zahnle 1994, Svetsov *et al.* 1995, Svetsov 1995) show that the deformation and disruption of a fluid impactor turned out to be more complex than simple semianalytical models predicted. However, there is fairly good agreement with these predictions in parameters such as the growth of the effective transversal radius, decrease of the mean velocity due to drag, and the energy release along the trajectory.

Pancake models are inappropriate for small impactors broken up only into several fragments. There is a transition to a regime such that separate fragments diverge (Passey and Melosh 1980, Melosh 1989, Artem'eva and Shuvalov 1996) and then fall individually. The famous Lost City meteorite is an example of such small impactors. Transition conditions are still in question. Below we deal mainly with impactors with kinetic energy above 0.1 kt TNT, i.e., larger than about 1 m in size, which is, according to analytical estimates of Svetsov *et al.* (1995), in the transition range. Nevertheless, our attempts to treat the flashes registered by satellites in the framework of standard meteor theory equations failed—rapid growth of radiation energy was inconsistent with the model of single body with constant radius (Svetsov *et al.* 1995, Nemtchinov *et al.* 1996b). Moreover, Popova and Nemtchinov (1996a,b) have recently investigated meteor events registered by PN and EN systems (see, e.g., Ceplecha and McCrosky 1976, Ceplecha *et al.* 1993, Ceplecha 1987, 1994, 1996). The results of our simulations and that of the dynamical trajectory analysis of PN bolides by Ceplecha (1996) in most cases do not contradict each other. For instance, for the Lost City meteorite using the radiation radius technique, we have obtained mass in the range of 50 to 150 kg and integral luminous efficiency (in the panchromatic passband) of the order 1% (Popova and Nemtchinov 1996a,b). That is rather close to the results of Ceplecha (1996), i.e., mass of about 160 kg and integral luminous efficiency of the order 1%. Our analysis of PN bolides with initial masses from 25 up to 1250 kg shows increase in integral luminous efficiency with velocity from about 1 to about 5% for velocities from 12–13 km/s to 21–23 km/s, respectively, in accordance with formulas (14) and (15). Applicability of our model to these rather small

meteoroids for approximating their characteristics may be explained by the fact that the duration of the flash associated with the breakup is proportional to the size of the body and for small bodies is small in comparison to the total duration of luminous flight. The larger the body, the larger the role of the flash associated with breakup. But the larger the meteoroid, the higher its probability of being disintegrated into a large number of fragments, and hence behaving in accordance with the pancake model.

Recently, a bright bolide (Benesov) was registered in Europe (Borovicka and Spurny 1996). A major final flash occurred at an altitude of about 25 km. It is the largest of the best documented events and is especially interesting because a spectrum was obtained in addition to trajectory and light curve. Detailed analysis of this event, including comparison of the observed spectrum with the theoretical one, will be given elsewhere. We shall note here that there is no disagreement in general features between the theoretical analysis and the observational data.

Two models have been used—the pancake model and a model treating individual flight of fragments, progressively decreasing their size, and increasing their number after each breakup until the cloud of small fragments and vapor creating the final flash is treated in the framework of a pancake model. Estimates of masses obtained using these two models for PN and EN bolides usually do not deviate by more than a factor of two. In the case of Benesov bolide they agree even more and are about 2–3 t, thus giving a kinetic energy of about 140–200 t TNT. That is approximately the lower energy of the SN bolides under consideration. This fact provides an additional foundation for our estimates above this threshold.

The term luminous efficiency is more frequent in literature in reference to a differential luminous efficiency and classical theory of meteor phenomena assumes that the amount of emitted energy per unit time is proportional to the kinetic energy of the mass losses due to ablation (Bronsten 1983, Ceplecha 1996). This differential luminous efficiency has been widely used for determination of ground-based meteoroids parameters (for example, Prairie Network meteors (McCrosky *et al.* 1971, Ceplecha and McCrosky 1976)). More generally, a differential luminous efficiency may be defined as the fraction of meteoroid kinetic energy transformed into light radiated during the ablation and deceleration of a meteoroid in the atmosphere, i.e., as a fraction of total energy losses of the meteoroid (see Eq. (4)) (ReVelle 1979, 1980, ReVelle and Rajan 1979).

Recent analysis of Lost City bolide (Ceplecha 1996) allows us to conclude that values of differential luminous efficiencies accepted in the past were substantially underestimated. The newly derived values of luminous efficiencies are about 10 times larger than those previously used for computations of the published photometric masses of Prairie Network (Ceplecha and McCrosky 1976) so the parameters of brightest fireballs would be revised (Ceplecha 1996).

Values of differential luminous efficiencies obtained in our simulations for spectral range of ground-based observations (Golub' *et al.* 1997) are closer to revised values found in (Ceplecha 1996) and greater than those used in the past also in agreement with Ceplecha (1996). In the case of SN bolides, when only light curves are known we used integral luminous efficiency defined by Eq. (13).

5. ASSESSMENTS OF INDIVIDUAL SN EVENTS

Detectors on board the satellites register light power versus time. An altitude of the major breakup has at times been obtained using a companion locator or from infrared observation of sun-lit debris. One way to determine meteoroid characteristics is to get a best fit of $P_r(t)$ to the light curve. The main characteristics are initial mass M_0, initial effective radius R_0, velocity V_0, and angle of trajectory inclination ϑ_0. Indirect integration of the system of equations of meteoroid motion, ablation, and radiation, i.e., Eqs. (4) and (6)–(9), allows us to narrow the amount of probe variants. If we set a height at peak signal h_m and a velocity at the end of radiation impulse V_k as boundary conditions for this system of equations, the functions $M(t)$, $R(t)$, $V(t)$, and $h(t)$ can be found using only V_0 and ϑ_0 as initial data. A numerical solution can be found by iterative procedure. The values M_0 and R_0 at the beginning of the light signal follow from the numerical solution. A precise value of V_k is not of great importance to us because the main part of the numerical solution is not appreciably influenced by it. Coefficients C_H/Q and f_d are calculated beforehand and are considered as given functions of R, h, and V. Influence of C_D is small within a reasonable accuracy.

Having M_0 and R_0 from the solution, we can assess the initial density of the body, assuming that the meteoroid is not very elongated or very flattened. Such an assessment gives a criterion for a choice of acceptable initial values of V_0 and ϑ_0 because the density cannot be higher than that of iron and cannot be lower than about 1 g/cm^3 if the altitude of breakup is not very high.

Equations (10) and (11) can be used as the second criterion for the choice of acceptable initial data. It seems highly improbable that the meteoroid radius can increase at a rate after breakup higher than what follows from (10) and (11). If several large fragments appear after breakup, their relative velocity U obeys (11) (Passey and Melosh 1980, Melosh 1989) which is close to (10).

Finally, we can use conventional wisdom for analysis of any numerical solution. For example, strongly diminishing $R(t)$ at constant M seems very unlikely. A typical accept-

able numerical solution is shown in Fig. 4 for the 1 October 1990 event. For velocity $V = 15$ km/s and $\vartheta = 25^0$ this solution gives a range of initial densities appropriate for that of a compact chondrite body. The radius after breakup grows at a rate close to that which follows from the pancake models of Chyba *et al.* (1993) and Hills and Goda (1993). Varying velocities, angles, and masses, we could not obtain a credible solution fitting an iron or cometary impactor.

The results of assessments of meteoroid parameters in seven events are collected in Table III. The largest event is the 1 February 1994 one, and this is the only case when the initial velocity (24 km/s) and angle of trajectory (45^0) were determined in addition to the light curve (McCord *et al.* 1995).

At the preliminary stage of investigation we did not know the results of trajectory tracking but obtained a velocity range (15–20 km/s), angle of depression (45^0), and an energy (30–40 kt TNT) rather close to the values given in Table III.

In addition, the progressive-fragmentation model mentioned above was also used. We also performed calculations assuming that this meteoroid was not an H-chondrite, as it was supposed in (Tagliaferri *et al.* 1995), but an iron. For this event the results do not differ substantially, hence increasing the credibility of our approach, at least for the high-energy events.

It is seen that the estimates of meteoroid parameters are made within various ranges of predicted values. In some cases the light-curve data were insufficient to narrow substantially the predicted range of parameters. These are 94149 and 94350 events with the low energy of meteoroid. Errors at low signal levels make it impossible to distinguish the light power at the stage before breakup, which is needed to judge the initial radius of the meteoroids. Assessments in these cases are poorer than for other events. It is reasonable to use integral luminous efficiency for estimations in such situations.

For the 3 November 1994 (94307) event we do not know the altitude at peak intensity. However, the radiation energy, peak intensity, duration, and shape of the light curve, including decay rate, are quite similar to those of the 90274 event, except for minor details. It seems very probable that these impactors had the same parameters; however, the "end point" for the 94307 event is about 12 km. This probably means that in this pair of events some of the fragments reached altitudes much lower than the altitude at peak signal determined for the 90274 by a companion locator.

An integral luminous efficiency η_i is shown in Table III. It lies within the values of η obtained using the more accurate approach with the exception of the 15 April 1988 event, for which we predict high velocity (40–50 km/s), substantially higher than the mean velocity of asteroids.

It should be remarked that in the earlier work (Svetsov

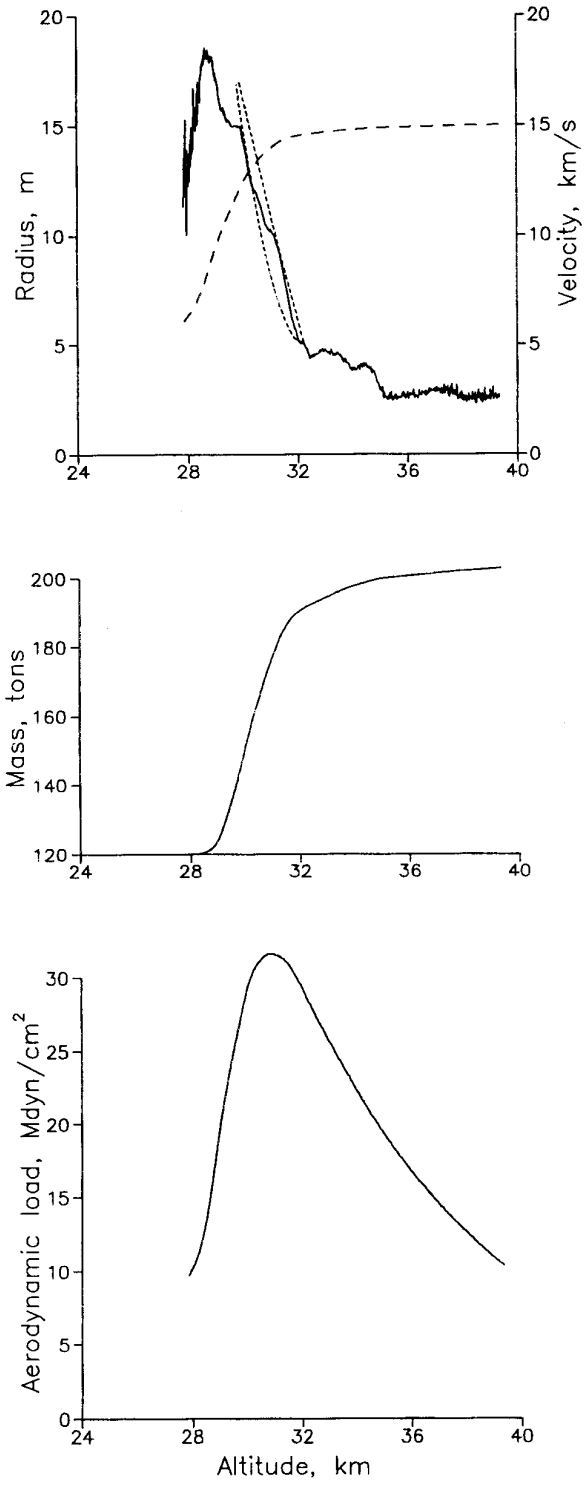

FIG. 4. Altitude dependence of effective radius (solid line, upper panel), velocity (dashed line, upper panel), mass, and aerodynamic load for the 90274 event as follows from numerical solution using H-chondrite coefficients. Altitude dependencies of radius after the breakup that follow from pancake models (10) and (11) are shown by dotted lines. It is assumed that $V_0 = 15$ km/s, $\vartheta_0 = 25^0$.

TABLE III
Parameters of SN Events Obtained from Simulations Using a Single-Body Model

Event	E (kt)	P_m (W/sr)	h_m (km)	E_0 (kt)	M_0 (ton)	V_0 (km/s)	η %	η_i %	Probable composition
88106 15 Apr. 1988	1.70	1.4×10^{12}	43	8–9	25–45	48–50	18–21	11	stony
90274 1 Oct. 1990	0.57	3.5×10^{11}	30	3–5	70–200	15–20	11–19	9.7	stony
91277 4 Oct. 1991	0.14	6.6×10^{10}	33	0.9	20	15–20	15	8.4	stony iron
94032 1 Feb. 1994	4.39	3.2×10^{12}	34, 21	31	400	24[a]	14	12.5	stony
94149 29 May 1994	0.090	9.9×10^{10}	34	0.6–2.5	2–140	<50	3.5–15	8.0	—
94307[b] 3 Nov. 1994	0.56	3.4×10^{11}	30[b]	3–5	70–200	15–20	11–19	9.7	stony
94350 16 Dec. 1994	0.0086	2.8×10^{10}	30	0.07–0.3	0.25–17	<40	3.3–14	5.9	—

Note. Here, E_r is the energy of the radiation impulse, P_m is the peak power of radiation, h_m is the height of breakup, E_0 is the kinetic energy of the body, M_0 is the mass, V_0 is the velocity, η is the luminous efficiency, and η_i is the integral luminous efficiency from approximation (16).

[a] Entry velocity is known from observational data.

[b] Using a similarity to 90274 in E_r, P_m, and a shape of the light curves.

et al. 1995, Nemtchinov *et al*. 1995, 1996a) we computed luminous efficiencies neglecting vapor radiation, and coefficients of heat transfer were borrowed from (Biberman *et al*. 1980). Because these coefficients were not self consistent, we varied the effective heat of ablation to avoid incredible numerical solutions. For this reason, the assessments for 90274, 91277, and 94032 are somewhat different from those made previously. However, the assessment of the 88106 event has not changed.

The energy of light impulse E_r measured from the satellites for 51 events is given in Table IV. Among these events listed in Table IV is the SN 94166 event, which ended in the fall of St. Robert meteorite (Brown *et al*. 1996). Analysis of cosmogenic nucleids has given estimates of the St. Robert meteoroid mass in the range of 700–4000 kg; the average value is 2300 kg, of which only about 100 kg landed in the form of small fragments. About 25 kg have been found. The mass of the largest of the 17 meteorites is only 6.5 kg, demonstrating the high degree of fragmentation typical for rather large meteoroids. IR observations from satellites led to the conclusions that the meteoroid began to disintegrate at an altitude of about 37.5 km and detonated at an altitude of 36.2 ± 1.5 km. The measured velocity at these altitudes was about 12 km/s.

The most probable initial velocity is 13 km/s (Brown *et al*. 1996). Assuming this velocity and using the average mass mentioned above, the initial kinetic energy is about 3.1×10^{11} J, which is equivalent to the energy of 78 t TNT. The integral luminous efficiency is 4%. These values only deviate from those in Table IV by 20–25%.

6. ENERGY–FREQUENCY DISTRIBUTION

Most of the events under consideration have been detected in the second half of 1994, 1995 and the first three months of 1996. We should note that systematic observations in the Western Hemisphere by the current detection system began in mid-1994 (Spalding 1996), so the duration of these systematic observations is about 22 months. Worldwide observations have been intermittent since December 1994. Systematic worldwide observations began in June 1996 and their results are not included in Table IV.

We divided all the energy range into bins, the kinetic energy ranging in each bin over a factor of four. The number of events per energy bin is presented in Fig. 5.

The number of detected bolides during 22 months of observations (from 3 June 1994 till the end of March 1996) is 14 in the energy bin of 0.06–0.25 kt TNT (two events were detected in 1993 when observations were not systematic). In the range of energies from 0.25 to 1 kt TNT the number of events is 16 (and none were detected in the previous years). Introducing a coefficient which takes into account incomplete observation in the Eastern Hemisphere (i.e., 1.46) and the ratio of one year to the duration of the observational period (i.e., 0.545), the number of impacts per year is 0.80 times the number of the detected events in 22 months. Therefore, the number of the impacts per Earth and per year is 11.2 and 12.8, respectively, in the above-mentioned energy bins.

In the bin of 1 to 4 kt TNT, 6 events were detected during the period of systematic observations and one was

TABLE IV

Assessment of Kinetic Energy of Bolides E_0 Using Theoretical Values of Integral Efficiencies η_i and Detected Energy of the Light Flashes E_r

Bolide data	P_m (W/sr)	E_r (kt)	η_i (%)	E_0 (kt)
88106	1.42×10^{12}	1.79	10.7	15.9
90274	3.53×10^{11}	0.57	9.7	5.88
91277	6.56×10^{10}	0.14	8.4	1.66
93304[a]	6.32×10^{9}	0.0095	5.95	0.16
93333	1.05×10^{10}	0.0063	5.58	0.11
94032	3.17×10^{12}	4.39	11.5	38.0
94149	9.90×10^{10}	0.090	8.00	1.12
94154	1.56×10^{11}	0.12	8.26	1.45
94166[b]	4.00×10^{9}	0.0031	4.93	0.063
94227	2.71×10^{10}	0.043	7.33	0.587
94265	6.50×10^{10}	0.016	6.53	0.244
94281	2.20×10^{10}	0.0157	6.51	0.241
94293	1.41×10^{10}	0.021	6.68	0.314
94300	8.42×10^{10}	0.077	7.86	0.979
94305	2.43×10^{11}	0.36	9.26	3.87
94307	3.39×10^{11}	0.56	9.67	5.79
94341	8.28×10^{9}	0.0019	4.49	0.043
94347	1.13×10^{10}	0.0029	4.87	0.059
94350	2.76×10^{10}	0.0086	5.86	0.147
95002	7.50×10^{9}	0.0071	5.79	0.123
95004	1.93×10^{10}	0.044	7.35	0.598
95010	9.00×10^{9}	0.006	5.63	0.106
95018	3.25×10^{10}	0.022	6.72	0.327
95047A	1.50×10^{10}	0.0042	5.21	0.081
95047B	1.00×10^{10}	0.014	6.31	0.222
95092	1.20×10^{10}	0.0060	5.63	0.106
95188	3.00×10^{10}	0.0333	7.20	0.463
95190	6.20×10^{10}	0.0595	7.73	0.770
95192	4.10×10^{10}	0.031	7.13	0.434
95217	1.80×10^{10}	0.0238	6.89	0.346
95218	2.40×10^{10}	0.013	6.35	0.206
95229	1.60×10^{10}	0.038	7.32	0.520
95236	2.70×10^{10}	0.0286	7.06	0.405
95252	7.50×10^{10}	0.119	8.36	1.420
95269	1.10×10^{10}	0.0029	4.96	0.058
95274	2.10×10^{10}	0.0083	5.93	0.140
95317	1.10×10^{10}	0.005	5.47	0.091
95322	6.50×10^{9}	0.0008	3.81	0.021
95323	5.50×10^{9}	0.0024	4.79	0.050
95329	2.10×10^{10}	0.0069	5.76	0.120
95343	4.70×10^{10}	0.0286	7.06	0.405
95356	7.80×10^{10}	0.107	8.26	1.297
95361	2.20×10^{10}	0.083	8.03	1.04
96015	6.30×10^{10}	0.067	7.83	0.851
96018	4.00×10^{10}	0.0029	4.96	0.058
96046	2.00×10^{10}	0.012	6.26	0.190
96047	1.70×10^{10}	0.0076	5.85	0.130
96073	3.30×10^{10}	0.055	7.65	0.716
96086	8.00×10^{9}	0.002	4.64	0.044
96089	3.00×10^{10}	0.021	6.77	0.309
96096	4.20×10^{10}	0.0286	7.06	0.405

[a] Noisy.

[b] Montreal, 10 Hz filtered, noisy, preliminary estimates of the energy have been corrected.

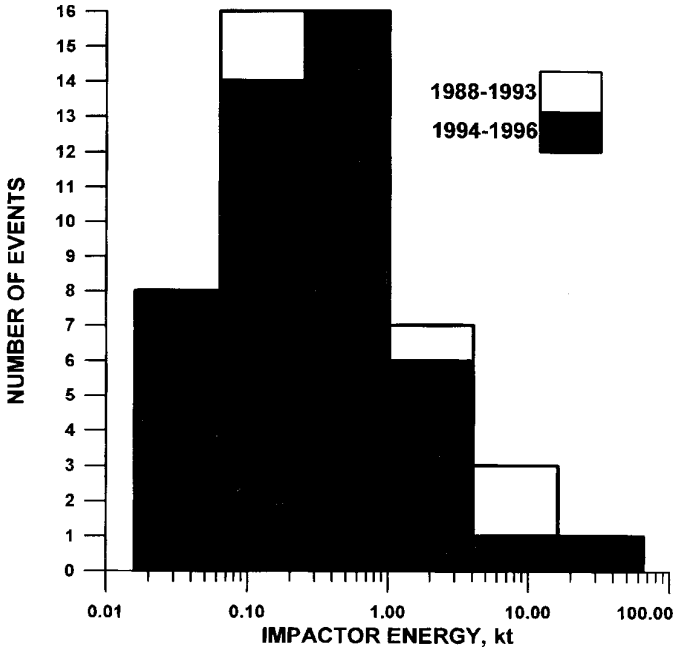

FIG. 5. Frequency of events versus energy of the impactors.

detected in 1991. The statistics are poor, but are still sufficient for obtaining estimates. Here, the number of impacts per year is 4.8.

In the energy bin of 0.064 to 0.16 kt TNT the number of events is also rather small, i.e., 8, and the average number of impacts per year is 6.4. This decrease in number for low-energy events is caused by the approach to the sensitivity limit of the satellite-based network which, according to Table IV, is about 20–40 t TNT for the energy and 5–8 GW/sr for the peak intensity.

In the energy bin 4–16 kt TNT only one event has been detected during 22 months of the systematic observations and two events were detected previously in 1988 and 1990. Therefore, the average number per year and per total surface of the Earth, i.e., 0.8, is determined with a very large uncertainty.

In the bin 16–64 kt TNT no impacts have been detected during 22 months, but the largest event (1 February 1994) with the energy of about 30–40 kt TNT occurred very close to this period (4 months earlier) and we have included this event in the determination of the cumulative number $N(E)$ of the bolides with energy larger than E. For this event we simply added four other months and assumed that the duration of the observational period is 30 months, so the average number of impacts in this energy range is 0.58 per year or once in 1.7 years. We calculated the cumulative number N of impacts per year over the entire surface of the Earth versus energy of impactor E for all the events detected in the period of the systematic observations. The dependence $N(E)$ is represented in Fig. 6 by open circles.

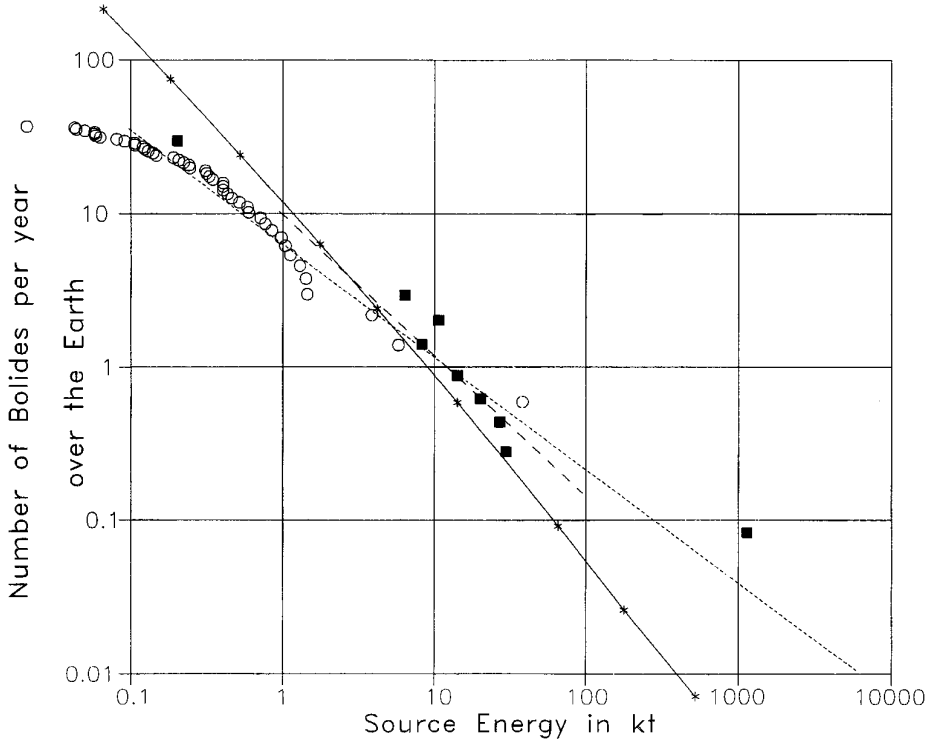

FIG. 6. Cumulative number of impacts onto the Earth per year versus energy of the impactor E_k kt TNT: (open circles) Detection by light sensors on board geostationary satellites taking into account the duration of the period of systematic observations (22 months) and a correction factor for intermittence of observations in Eastern Hemisphere, (black squares) observations by acoustic system (ReVelle 1996), (short dashed line) approximation of the acoustic observation data, (Dashed line) best estimate of the near-Earth object by Shoemaker (1983), (stars) distribution derived from lunar crater data (Neukum and Ivanov 1994).

The total energy released in the Earth's atmosphere per year in the energy range from 0.02 to 30 kt TNT is 55.7 kt TNT. The total number of the impacts per year per Earth in the same energy range is 36.5, thus the average energy of the impacts is 1.5 kt TNT. The largest annual event expected is about 10–15 kt TNT.

ReVelle (1995, 1996) has analyzed the energy–frequency distribution obtained from acoustic observations. These data are shown in Fig. 6 as black squares. We should note that the number of the events detected by such a system is rather small. The total number of the events detected by optical system and used in Fig. 6 is about 5 times larger than for the acoustic system.

ReVelle (1995) has derived the following approximation for the energy–frequency distribution from the acoustic observation

$$N(E) = 7.2E^{-0.7}, \tag{17}$$

where N is the cumulative number of events with energy larger than E, and E is the kinetic energy in kt TNT. This curve is also given in Fig. 6.

Comparing data from the acoustic and optical systems, one can see that they are rather close to each other. The relation (17) may be used for estimates. It follows from (17) that the differential number of events rapidly grows with a decrease of the sensitivity limit E_s as $E_s^{-1.7}$, as most of the impacts involve low-energy impactors. The total energy released in the atmosphere grows with the duration of the observational period. The high-energy events having low probability will be eventually encountered in reality.

According to formula (17) the probability of a 1 Mt event is once in about 17 years. A 1 Mt event has been recorded during 12 years of observations via the acoustical system (ReVelle 1995, 1996). During almost 2 years of systematic observations by satellites not a single event with energy as large as 0.1–1 Mt has been detected as yet.

Optical system data fit formula (17) and a 1 Mt event are anticipated to be registered in the coming 15–20 years, but there is a large amount of uncertainty due to poor statistics for large energy events. The frequency of events in the range 0.25–4 kt will probably not be substantially changed in the future as the number of the detected events in this range is already rather large (i.e., 22), and this interval of energies is rather far from the sensitivity limit. In this energy range the total number of impacts per year

and per Earth is 17.6 and the released energy is 18.6 kt TNT. Thus the average energy per impact is about 1 kt TNT.

Let us compare the energy–frequency distribution obtained as the result of analysis of the light impulse detected by satellites with previously published estimates.

Usually, hazards due to comets and asteroids have been analyzed for rather large cosmic bodies, i.e., with the initial kinetic energy more than 3×10^5 Mt (Morrison *et al.* 1994). But impacting cosmic bodies with energies about 10–30 Mt (Tunguska class objects) may also be dangerous (see, e.g., Adushkin and Nemtchinov 1994, Hills *et al.* 1994). In the energy range less than 30 Mt a smooth curve of the cumulative energy–frequency for impacts in the Earth has been presented by Morrison and Chapman (1994). This curve is the so-called ''best estimate'' from Shoemaker (1983) based primarily on lunar crater data. Recently, it was argued (Rabinowitz 1993, 1994, Rabinowitz *et al.* 1994) that the Spacewatch observations (Scotti 1994, Carusi *et al.* 1994) show a substantial enhancement of the population of near-Earth objects in this size range. Here we have plotted the best estimate, not taking into account this probable enhancement, and have used the approximation

$$N = 10E^{-0.87}, \tag{18}$$

where E is the kinetic energy in kt TNT. This expression gives the probability of a 30 Mt event once in 300 years and of a 1 Mt event once in 40 years. This formula has been presented in Fig. 6. One can see that this approximation also correlates with observational data of the acoustical and optical systems rather well, except for the 1 Mt event of the acoustical system.

Ceplecha (1992) has constructed a mass–frequency distribution for a very wide range of meteoroid masses. He used data both from ground-based meteoroid observations (Prairie and European Networks) and from astronomical observations (through telescopes). In his set of meteor data the largest bolide had a mass of about 2 t and energy of about 100 t TNT, but mainly much smaller bolides were used. He also used an interpolation between these two sets of experimental data. We should note that intervals with masses larger than 1–3 t have not been covered by ground-based photographic networks at all. In the range of masses from 1×10^{-2} kg to 1×10^6 kg, Ceplecha (1992) assumed a constant power law similar to (17) or (18) but with another exponent, i.e., (-0.55). This exponent is much smaller than that in the approximation (17) or (18) and means that the frequency of impacts decreases with the energy of the impactor more slowly than in formulas (17) and (18).

To convert mass–frequency distribution by Ceplecha (1992) into the energy–frequency distribution we have assumed as the typical velocity of the impactor $V = 17.8$ km/s. This gives us the following conversion relationship: the kinetic energy is equivalent to the chemical energy released in the explosion of 36 t TNT for a meteoroid with a mass of 1 t.

We have compared satellite observations with best estimates of Shoemaker (1983) and data in Morrison and Chapman (1994) not taking into account the so-called enhancement for 5–50-m bodies (Rabinowitz 1993, 1994, Rabinowitz *et al.* 1993, 1994) and obtained rather good agreement. This does not necessarily imply that such enhancement does not exist. First, the precision of energy determination is still not very good. According to formula (17) or (18), if we change the energy by a factor of two the differential probability dN/dE may change by a factor of about 3–4. Second, a systematic bias may exist if the velocity in the near-Earth asteroid belt is lower than the average velocity of impactors and if the resultant luminous efficiency for such meteoroids is smaller than assumed in (16). To decrease the uncertainty by upgrading the Satellite Network system, a priority task would be to include trajectory tracking. Some other peculiar features of the near-Earth asteroid belt population may be reducing the number of detections by the satellites optical system. There are several ways to improve the system so as to prevent such detection losses, e.g., using the light sensors in differential wavelength bands. Of course, theoretical models should be improved too. On the other hand, the very large enhancement claimed by Rabinowitz (1994), i.e., by a factor of 40 or even larger, seems to contradict observations via satellites.

According to the estimate of (Ceplecha 1992) for mass greater than 1 t (and kinetic energy of about 36 t TNT), $N = 10^3$ events per year, which is much larger than the estimate according to (17) and (18). Furthermore, the exponent in the power law given by Ceplecha (1992) is also rather small and the discrepancy with observational data increases with initial energy of the meteoroid.

Recently, a new estimate has been given by Ceplecha *et al.* (1996) using data of the satellite network observations and the range of empirical values of luminous efficiencies determined by the analysis of Prairie Network bolides. Luminous efficiencies varied in a wider range than we assumed (from 1.4 to 10%). A smaller number of the events, i.e., only 21, have been used in Ceplecha *et al.* (1996) which increases the uncertainty of the energy–frequency distribution. The cumulative number of events in Ceplecha *et al.* (1996) is still rather high, about 10 per year per Earth for a 30 kt TNT event, while only one such event has actually been detected in about 2 years.

Let us compare the energy–frequency distribution derived from satellite observations directly with that from lunar crater data (Neukum and Ivanov 1994), not with its approximation by a power law (18). These data were approximated by a polynomial of 12th degree with coefficients given in Neukum and Ivanov 1994) and are repre-

sented in Fig. 6 by stars. Satellite data also agree with the original lunar crater record. A kink in the energy–frequency curve is clearly seen for all the observations, including the acoustic data if we exclude the isolated 1 Mt event, for which the real interval between the events is not known.

It seems also that assumption on the average time interval between the 30 kt events, i.e., 30 months, has been substantially underestimated. Using the lunar record curve one may anticipate this interval to be as large as 3 to 5 years.

The wavy character of the size–frequency distribution of asteroids in the asteroidal belt, i.e., deviation from a simple power law, has not only been found by astronomical observations through telescopes, but has also been predicted by a theory of cosmic bodies collisions and fragmentation (see, e.g., Farinella *et al.* 1982, Campo Bagati *et al.* 1994). Monte Carlo simulations have shown that for asteroids such a kink exists for bodies with diameters about 30 km. Recently, an evolution of the size distribution has been studied by solving the integral equation for number density of cosmic bodies (Dohnanyi 1969). A special numerical technique (de Niem 1996, personal communication) has permitted study of the distribution for a very wide range of sizes—from 1 mm to 1000 km. A clear kink in the distribution curve has been found for 1–10 m bodies just in the place that follows from the lunar crater record (Neukum and Ivanov 1994) and from the satellite observations of flashes caused by the meteoroids entering the atmosphere. Increase in the slope of the energy–frequency curve for energies larger than about 5–6 kt TNT increases the average interval between such impacts.

7. CONCLUSIONS

Energy–frequency distribution of meteoroid impacts into the Earth's atmosphere have been obtained using data on 51 light flashes detected by satellite-based sensors. The duration of systematic observations is 22 months—from mid 1994 until March 1996. Theoretical values of luminous efficiencies based on results of radiation hydrodynamic simulations and calculations of the vapor spectral opacities have been determined. The cumulative number of impacts per the Earth and per year for meteoroids with kinetic energy above 0.25 up to 1 kt TNT and from 1 to 4 kt TNT is 19 and 6.2, respectively.

These numbers are approximately a factor of two lower than that of the lunar crater data. For energies of about 3–10 kt TNT all the observations (by satellite-based light sensors, by acoustical system, and by lunar crater record analysis) set the number of impacts at about 2–3 per year and per Earth. Extrapolation of this number for a 1 Mt event gives an average time interval between such events with a great scatter. Using approximation (17) or (18) we may expect the 1 Mt event once in 17 or 40 years. Acoustical systems detected one such event in 12 years of observations. Satellite optical sensors have not detected such an event yet, due to a shorter time of observations. It is necessary to continue the observations to obtain an energy–frequency curve that is statistically more well founded, especially for rather rare high-energy events; such a curve would then make it possible to predict the probability of truly energetic impacts with more certainty.

The number of events detected by the satellite optical system over two years of observations agrees with the lunar record data over approximately 400 million years. This agreement implies that the impact rate in the modern epoch does not substantially differ from the average value over a much longer period of time.

ACKNOWLEDGMENTS

We express our gratitude for valuable discussions to G. Neukum, D. de Niem, H. Rickman, and P. Weissman. We gratefully acknowledge the reviews by T. McCord and P. Brown and helpful criticism of the anonymous referee.

REFERENCES

Adushkin, V. V., and I. V. Nemtchinov 1994. Consequences of impacts of cosmic bodies on the surface of the Earth. In *Hazards Due to Comets and Asteroids* (T. Gehrels, Ed.), pp. 721–778. Univ. of Arizona Press, Tucson.

Artem'eva, N. A., and V. V. Shuvalov 1996. Interaction of shock waves during the passage of a disrupted meteoroid through the atmosphere. *Shock Waves* **5,** 359–367.

Avilova, I. V., L. M. Biberman, V. S. Vorob'ev, V. M. Zamalin, G. A. Kobzev, A. N. Lagar'kov, A. H. Mnatsakanyan, and G. E. Norman 1970. In *Optical Properties of the Hot Air* (L. M. Biberman, Ed.), p. 320. Nauka, Moscow.

Ayers, W. G., R. E. McCrosky, and C.-Y. Shao 1970. Photographic observations of 10 artificial meteors. *Spec. Rept. Smithsonian Astrophys. Observ.* **317**, 45.

Baldwin, B. S., and V. Sheaffer 1971. Ablation and breakup of large meteoroids during atmospheric entry. *J. Geophys. Res.* **76,** 4653–4668.

Biberman, L. M., S. Ya. Bronin, and M. V. Brykin 1980. Moving of a blunt body through the dense atmosphere under conditions of severe aerodynamic heating and ablation. *Acta Astronautica* **7,** 53–65.

Borovicka, J., and P. Spurny 1996. Radiation study of two very bright terrestrial bolides. *Icarus* **121,** 484–510.

Bronsten, V. A. 1983. *Physics of Meteoric Phenomena*, Reidel, Dordrecht.

Brown, P., A. R. Hildebrand, D. W. E. Green, D. Page, C. Jacobs, D. ReVelle, E. Tagliaferri, J. Wacker, and B. Wetmiller 1996. The fall of the St. Robert meteorite. *Meteoritics Planet. Sci.* **31,** 502–517.

Campo B. A., A. Cellino, D. R. Davis, P. Farinella, and P. Paolicchi 1994. Wavy size distribution for collisional systems with a small cutoff. *Planet. Space Sci.* **42,** 1079–1092.

Carusi, A., T. Gehrels, E. F. Helen, B. G. Marsden, K. S. Russel, C. S. Shoemaker, E. M. Shoemaker, and D. I. Steel 1994. Near-Earth objects: Present search programs. In *Hazards Due to Comets and Asteroids* (T. Gehrels, Ed.), pp. 127–147. Univ. of Arizona Press, Tucson.

Ceplecha, Z. 1987. Geometric, dynamic, orbital and photographic data on meteoroids from photographic fireball networks. *Bull. Astron. Inst. Czech.* **38,** 222–234.

Ceplecha, Z. 1992. Influx of interplanetary bodies onto Earth. *Astron. Astrophys*. **263,** 361–366.

Ceplecha, Z. 1994. Meteoroid properties from photographic records of meteors and *fireballs*. In *Asteroids, Comets, Meteors 1993* (A. Milani, M. D. Martino, and A. Cellino, Eds.), pp. 343–356. IAU Symposium No. 160, Kluwer, Dordrecht.

Ceplecha, Z. 1996a. Differential and total luminous efficiency of fireballs. *Int. Conf. on Asteroids, Comets and Meteors. ACM-96, Versaille 8–12 July, 1996*. p. 29 [Abstract]

Ceplecha, Z. 1996b. Luminous efficiency based on photographic observations of Lost-City fireball and implications to the in flux of interplanetary bodies onto Earth. *Astron. Astrophys*. **311,** 329–332.

Ceplecha, Z., and R. E. McCrosky 1976. Fireball and heights: A diagnostic for the structure of meteoric material. *J. Geophys. Res*. **81,** 6257–6275.

Ceplecha, Z., P. Spurný, J. Borovicka, and J. Keklikova 1993. Atmospheric fragmentation of meteoroids. *Astron. Astrophys*. **279,** 615–626.

Ceplecha, Z., R. E. Spalding, C. Jacobs, and E. Tagliaferri 1996. Sizes and masses of satellite observed meteoroids. *Proc. Comet Day II* (*5th Int. Conf. Space—96*)*, June 1–6, 1996, Albuquerque, NM.*

Cherniy, G. G. 1959. *A Hypervelocity Gas Flow*. Fizmatgiz, Moscow.

Chyba, C. F., P. J. Thomas, and K. J. Zahnle 1993. The 1908 Tunguska explosion: Atmospheric disruption of a stony asteroid. *Nature* **361,** 40–44.

Dohnanyi, J. S. 1969. Collisional model of asteroids and their debris. *J. Geophys. Res*. **74,** 2531–2554.

Farinella, P., P. Paolicchi, and V. Zappala 1982. The asteroids as the outcomes of catastrophic collisions. *Icarus* **52,** 409–433.

Givens, J. J., and W. A. Page 1971. Ablation and luminosity of artificial meteors. *J. Geophys. Res*. **76,** 1039–1054.

Glasstone, S., and P. Dolan 1977. *The Effects of Nuclear Weapons*. U.S. Dept. of Defense and U.S. Dept. of Energy. U.S. Government Printing Office, Washington, DC.

Golub', A. P., I. B. Kosarev, I. V. Nemtchinov, and V. V. Shuvalov 1996. Emission and ablation of a large meteoroid in the course of its motion through the Earth's atmosphere. *Solar System Res.* **30,** 183–197.

Golub', A. P., I. B. Kosarev, I. V. Nemtchinov, and O. P. Popova 1997. Emission spectra of bright bolides. *Solar System Res.* **31,** 85–98.

Hayes, W. D., and R. F. Probstein 1959. *Hypersonic Flow Theory*. Academic Press, New York.

Hills, J. G., and M. P. Goda 1993. The fragmentation of small asteroids in the atmosphere. *Astron. J*. **105,** 1114–1144.

Hills, J. G., I. V. Nemtchinov, S. P. Popov, and A. V. Teterev 1994. Tsunami generated by small asteroid impacts. In *Hazards Due to Comets and Asteroids* (T. Gehrels, Ed.), pp. 779–789. Univ. of Arizona Press, Tucson.

Jarocewich, E. 1990. Chemical analyses of meteorites: A compilation of stony and iron meteorite analyses. *Meteoritics* **25,** 323–337.

Kosarev, I. B., T. V. Loseva, and I. V. Nemtchinov 1996. Vapor optical properties and ablation of large chondrite and ice bodies in the Earth's atmosphere. *Solar System Res*. **30,** 265–278.

Kuznetsov, N. M. 1965. *Thermodynamic Functions and Shock Adiabats for Air at High Temperatures*. Mashinostroyenie, Moscow.

McCord, T. B., J. Morris, D. Persing, E. Tagliaferri, C. Jacobs, R. Spalding, L. A. Grady, and R. Schmidt 1995. Detection of a meteoroid entry into the Earth's atmosphere on February 1, 1994. *J. Geophys. Res*. **100,** 3245–3249.

McCrosky, R. E., A. Posen, G. Schwartz, and C.-Y. Shao 1971. Lost-City meteorite—Its recovery and a comparison with other fireballs. *J. Geophys. Res*. **76,** 4090–4108.

Melosh, H. J. 1989. *Impact Cratering: A Geological Process*. Oxford Univ. Press, New York/Clarendon Press, Oxford.

Morrison, D., C. R. Chapman, and P. Slovic 1994. The impact hazard. In *Hazards Due to Comets and Asteroids* (T. Gehrels, Ed.), pp. 59–91. Univ. of Arizona Press, Tucson.

Nemtchinov, I. V., O. P. Popova, V. V. Shuvalov, and V. V. Svetsov 1994. Radiation emitted during the flight of asteroids and comets through the atmosphere. *Planet. Space Sci*. **42,** 491–506.

Nemtchinov, I. V., O. P. Popova, V. V. Shuvalov, and V. V. Svetsov 1995. On photometric masses and radiation sizes of large meteoroid. *Solar System Res.* **29,** 133–150.

Nemtchinov, I. V., T. V. Loseva, and A. V. Teterev 1996a. Impacts into oceans and seas. *Earth, Moon, Planets* **72,** 405–418.

Nemtchinov, I. V., V. V. Svetsov, A. P. Golub', I. B. Kosarev, O. P. Popova, V. V. Shuvalov, R. E. Spalding, C. Jacobs, and E. Tagliaferri 1996b. Assessment of kinetic energy of meteoroids detected by satellite based light sensors. *Proc. Comet Day II* (*5th Int. Conf. Space—96*)*, Albuquerque, NM.*

Neukum, G., and B. A. Ivanov 1994. Crater size distributions and impact probabilities on Earth from lunar, terrestrial-planet, and asteroid cratering data. In *Hazards Due to Comets and Asteroids* (T. Gehrels, Ed.), pp. 359–416. Univ. of Arizona Press, Tucson.

Passey, Q. R., and H. J. Melosh 1980. Effects of atmospheric breakup on crater field formation. *Icarus* **42,** 211–233.

Popova, O. P., and I. V. Nemtchinov 1996a. Estimates of fireballs mass based on light curves. *Int. Conf. on Asteroids, Comets and Meteors, ACM-96. 8–12 July, 1996, Versailles, France*. [Abstract]

Popova, O. P., and I. V. Nemtchinov 1996b. Estimates of PN bolide characteristics based on the light curves. *Meteoritics Planet. Sci*. **31,** P.A110. [supplement]

Rabinowitz, D. 1993. The size distribution of the Earth-approaching asteroids. *Astrophys. J*. **407,** 412–417.

Rabinowitz, D. 1994. The size and shape of the near-Earth asteroid belt. *Icarus* **111,** 364–377.

Rabinowitz, D., E. Bowell, E. Shoemaker, and K. Muinonen 1994. The population of Earth-crossing asteroids. In *Hazards Due to Comets and Asteroids* (T. Gehrels, Ed.), pp. 285–313. Univ. of Arizona Press, Tucson.

Rabinowitz, D., T. Gehrels, J. V. Scotti, R. S. McMillan, M. L. Perry, W. Wisniewski, S. M. Larson, E. S. Howell, and B. E. A. Mueller 1993. Evidence of a near-Earth asteroid belt. *Nature* **363,** 704–706.

Remo, J. L. 1994. Classifying and modeling NEO material properties and interactions. In *Hazards Due to Comets and Asteroids* (T. Gehrels, Ed.), pp. 551–596. Univ. of Arizona Press, Tucson.

ReVelle, D. O. 1979. A quasi-simple ablation model for large meteorite entry: Theory vs observations. *J. Atmos. Terr. Phys*. **41,** 453–473.

ReVelle, D. O. 1980. A predictive macroscopic integral radiation efficiency model. *J. Geophys. Res*. **85,** 1803–1809.

ReVelle, D. O. 1995. Historical detection of atmospheric impacts by large bolides using acoustic-gravity waves. *Int. Conf. on Near-Earth Objects. April 24–26, 1995*. The Explorers Club and United Nations Office for Outer Space Affairs, New York City. [abstracts]

ReVelle, D. O. 1996. Acoustic efficiency analysis using infrasound from NEOs. *Proc. Comet Day II* (*5th Int. Conf. Space-96*)*, June 1–6, 1996, Albuquerque, NM*.

ReVelle, D. O., and R. S. Rajan 1979. On the luminous efficiency of meteoritic fireballs. *J. Geophys. Res*. **84,** 6255–6262.

Reynolds, D. A. 1992. Fireball observation via satellite. In *Proc. Near-Earth-Object Interception Workshop* (G. H. Canavan, J. C. Solem, and J. D. G. Rather, Eds.), pp. 221–226. Los Alamos.

Scotti, J. V. 1994. Computer aided near-Earth object detection. *Asteroids, Comets, Meteors 1993* (A. Milani, M. D. Martino, and A. Cellino, Eds.), pp. 17–30. IAU, Kluwer, Netherlands.

Shoemaker, E. 1983. Asteroids and comet bombardment of the Earth. *Annu. Rev. Earth Planet. Sci.* **11,** 461–494.

Spalding, R. E. 1996. Satellite visible-light sensors bolide detection. *Meteoroid Impact Workshop, Sandia National Laboratories, June 4–7, 1996, Albuquerque, NM*.

Svetsov, V. V. 1994. Explosions in the lower and middle atmosphere: The spherically symmetrical stage. *Combust. Explosion Shock Waves* **30,** 696–707.

Svetsov, V. V. 1996a. Where have the debris of the Tunguska meteoroid gone? *Solar System Res.* **30,** 378–390.

Svetsov, V. V. 1996b. Total ablation of the debris from the 1908 Tunguska explosion. *Nature* **383,** 697–699.

Svetsov, V. V., I. V. Nemtchinov, and A. V. Teterev 1995. Disintegration of large meteoroids in the Earth's atmosphere: Theoretical models. *Icarus* **116,** 131–153.

Tagliaferri, E. 1993. Asteroid detection by space-based sensors. *Erice Int. Seminar, The Collision of an Asteroid or Comet with the Earth*.

Tagliaferri, E. 1996. Satellite observations of large meteoroid impacts. *Meteoroid Impact Workshop, Sandia National Laboratories, June 4–7, 1996, Albuquerque, NM*.

Tagliaferri, E., R. Spalding, C. Jacobs, S. P. Worden, and A. Erlich 1994. Detection of meteoroid impacts by optical sensors in Earth orbit. In *Hazards Due to Comets and Asteroids* (T. Gehrels, Ed.), pp. 199–220. Univ. of Arizona Press, Tucson.

Zahnle, K. J. 1992. Airburst origin of dark shadows on Venus. *J. Geophys. Res.* **97,** 10,243–10,255.